Automatic Polyp Detection from Endoscope Image using Likelihood Map based on Edge Information

Yuji Iwahori[1], Hiroaki Hagi[1], Hiroyasu Usami[1], Robert J. Woodham[2], Aili Wang[3], M. K. Bhuyan[4] and Kunio Kasugai[5]

[1]*Department of Computer Science, Chubu University, Kasugai, 487-8501, Japan*

[2]*Department of Computer Science, University of British Columbia, Vancouver, B.C., V6T 1Z4, Canada*

[3]*Higher Education Key Lab for Measuring & Control, Harbin University of Science and Technology, Harbin, China*

[4]*Department of Electronics and Electrical Engineering, Indian Institute of Technology Guwahati, Guwahati, 781039, India*

[5]*Department of Gastroenterology, Aichi Medical University, Nagakute, 480-1195, Japan*

iwahori@cs.chubu.ac.jp, {hagi_g, usami}@cvl.cs.chubu.ac.jp, woodham@cs.ubc.ca, aili925@hrbust.edu.cn, mkb@iitg.ernet.in, kuku3487@aichi-med-u.ac.jp

Keywords: Polyp Detection, Endoscope Image, Likelihood, HOG, Random Forests.

Abstract: An endoscope is a medical instrument that acquires images inside the human body. This paper proposes a new approach for the automatic detection of polyp regions in an endoscope image by generating a likelihood map with both of edge and color information to obtain high accuracy so that probability becomes high at around polyp candidate region. Next, Histograms of Oriented Gradients (HOG) features are extracted from the detected region and random forests are applied for the classification to judge whether the detected region is polyp region or not. It is shown that the proposed approach has high accuracy for the polyp detection and the usefulness is confirmed through the computer experiments with endoscope images.

1 INTRODUCTION

Medicine is an important area as the application of computer vision. Endoscopy allows medical practitioners to observe the interior of hollow organs and other body cavities in a minimally invasive way. Diagnosis involves both shape detection and the assessment of tissue state. Here, we consider a general purpose endoscope, of the sort still most widely used in medical practice. There are many different kinds of polyp shape and size in endoscope images. Polyps are usually found via endoscopy but polyps can be missed. The main factor to find polyp depends on the empirical skill of medical doctors. Automatic detection of polyps, with high accuracy, is an important aid to medical practice. Diagnosis typically requires polyp removal and biopsy.

Some previous approaches (Ameling et al., 2009) (Karkanis et al., 2003) (Iakovidis et al., 2005) are patch-based approaches which introduce features of Color Wavlet Covariance (CWC), Local Binary Pattern (LBP), Gray-Level Co-Occurrence Matrix (GLCM), which is used for the texture analysis, respectively. Another approach (Alexandre et al., 2008) learns color and *xy* position coordinates partitioned in the local window, then classifies if a polyp is included or not in the each region. These are patch-based approaches and extract features and perform classification. Patch-based approach may include the problem that detection ratio depends on patch size and position of polyp.

Paper (Li and Meng, 2011) uses capsule endoscope images as input and extracts the Rotational Invariant Uniform Local Binary Pattern (RIULBP), and statistical value are obtained from intensity histogram as texture features. Classifier is designed to learn these features for the polyp detection. The approach has some difficulty in detecting small polyp with non-textures.

On the other hand, the geometric feature is used in the approach (Hwang et al., 2007) so that polyp appears with ellipse form in general. The approach detects polyp with only the ellipse fitting without any learning. Geometrical feature based approach is robust to the small polyp, but some segmentation is necessary to detect polyps with edge information, that is, the detection performance depends on the level of edge extraction.

Iwahori, Y., Hagi, H., Usami, H., Woodham, R., Wang, A., Bhuyan, M. and Kasugai, K.
Automatic Polyp Detection from Endoscope Image using Likelihood Map based on Edge Information.
DOI: 10.5220/0006189704020409
In *Proceedings of the 6th International Conference on Pattern Recognition Applications and Methods (ICPRAM 2017)*, pages 402-409
ISBN: 978-989-758-222-6

Another approach proposed in paper (Iwahori et al., 2013) is Hessian Filter based approach, where Hessian filter emphasizes the blob-like structure and extracts some polyp candidates with segmentation. Some texture-based features extracted from each polyp candidate region are classified with SVM and judged whether the candidate region is polyp region or not. This approach is not patch-based but many regions can be extracted as the polyp candidate region. Each candidate region is classified using SVM as the 2nd step.

Paper (Bernal et al., 2015) extracts the edge with the valley which has smaller value of image intensity in comparison with the surrounding points. Polyp is detected by generating the map which has the larger value for the higher possibility of exist of the polyp based on the edge. This approach is reasonable, but the blood vessel is also extracted as edge. When the blood vessel has the similar shape as the edge or the image has many blood vessels, the approach has the problem.

This paper further improves the polyp detection problem to have the higher accuracy based on both edge-based features and shape-based features. The approach constructs reliable likelihood map on the polyp candidates and proposes an automatic detection of polyp with higher accuracy in classification.

2 AUTOMATIC POLYP DETECTION

Proposed approach generates the likelihood map using the edge information using the gradient which is obtained by multi-scale. The polyp candidate region is extracted using the likelihood map and classifier is applied to detect the polyp using SVM. Proposed approach is explained here.

2.1 Removal of Specular Reflectance Component

Many specular reflectance components are observed in endoscope image and this specular reflectance component should be removed to detect the exact polyp. Proposed approach extracts the specular reflectance components (Shen and Cai, 2009) and interpolation is applied to the extracted region. The process is shown below.

First, the minimum value of RGB for each pixel is obtained using Eq.(1).

$$V_{\min}(x,y) = \min_i\{V_i(x,y)\} \tag{1}$$

where V represents the image, i represents the RGB channel, x and y represent image coordinates. Next, mean μ_v and standard deviation σ_v of $V_{\min}$ are obtained and threshold value T_v is determined using Eq.(2).

$$T_v = \mu_v + 0.5\sigma_v \tag{2}$$

Offset $\tau(x,y)$ is obtained using T_v by Eq.(3).

$$\tau(x,y) = \begin{cases} T_v & \text{if } V_{\min}(x,y) > T_v \\ V_{\min}(x,y) & otherwise \end{cases} \tag{3}$$

Next, specular reflectance component β is obtained using $V_{\min}$ and offset τ.

$$\beta(x,y) = V_{\min}(x,y) - \tau(x,y) \tag{4}$$

The region which has the larger value of obtained β is interpolated by the inpainting. Result in which the specular reflectance component was removed from the original endoscope image is shown in Fig.1.

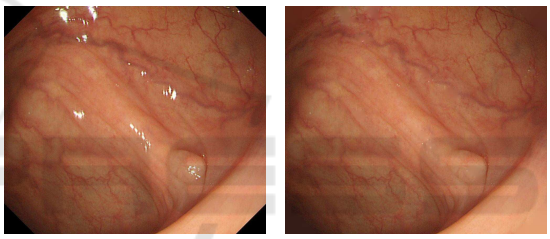

(a) Original Image (b) Removal Image

Figure 1: Removal of Specular Reflectance Component.

2.2 Edge Detection

Proposed approach uses gradient of image intensity for edge detection. However, blurring sometimes occurs in endoscope video or noise and textures may affect edge detection. Firstly gaussian filter is applied to detect correct edge by reducing these effects.

Simple apply of edge detection for the endoscope image generates edges including polyp and other blood vessels. When edge detection is applied to polyp detection using edge shape, the operation sometimes becomes useless since blood vessel is detected as polyp candidate based on the shape information.

Proposed approach detects edge by varying the scale σ of Gaussian function for the convolution to reduce the detection of blood vessel. When the value of the scale σ is small, detailed edge including blood vessel is also detected except the polyp and inner lining, while when the value of the scale σ is large, rough edge is detected with the bold edge, instead blood vessel is not detected. The approach varies the scale σ,

reduces the detection of blood vessel as edge and prevents to become bold edge in the result image.

In addition, edge intensity E is obtained by multiplying these detected edge by edge which is obtained using morphology gradient processing which subtracts the image generated by the contraction process of morphology operation from the image generated by the expansion process of the morphology operation.

The procedures are shown as follows.

Step1. Gaussian function $G(x,y)$ is generated and its first directional derivatives $G_x(x,y)$ and $G_y(x,y)$ are obtained. Further, its second derivatives $G_{xx}(x,y)$ and $G_{yy}(x,y)$ are also obtained.

Step2. Image $L(x,y)$ and $G_{xx}(x,y)$, $G_{yy}(x,y)$ are convolved and derivatives $L_{xx}(x,y)$ and $L_{xx}(x,y)$ are obtained.

Step3. $L_{\max}$ is obtained from L_{xx} and L_{yy}.

$$L_{\max}(x,y) = \max(L_{xx}(x,y), L_{yy}(x,y)) \quad (5)$$

Step4. Repeat **Step2** to **Step4** by varying the scale σ of Gaussian function.

Step5. Sum of $L_{\max}$ obtained for each scale σ is obtained. Here n_s represents a number of different scale σ.

$$L_{\mathrm{sum}}(x,y) = \sum_{i}^{n_s} L_{\max,i}(x,y) \quad (6)$$

Step6. Morphology gradient processing is applied to the input image L and edge intensity E is obtained by multiplying L_{sum}.

2.3 Generation of Likelihood Map

Paper (Bernal et al., 2015) generates likelihood map based on edge shape and its intensity from the viewpoint of the condition that polyp edge is part of circular shape. Proposed approach tries to obtain the map which takes lower value for except polyp by adding the weight using the bright/dark color in the likelihood map generated by (Bernal et al., 2015). Procedure to generate likelihood map is shown as follows. Outline to generate likelihood map by the proposed approach is shown in Fig.2.

A circle with any size is generated, whose center is located at the interesting pixel p. Circle is divided into multiple regions with any value of degree. Maximum value $S_i^{\max}$ of edge intensity E is obtained for each divided region S_i. This operation is shown in Fig.2(a).

$$S_i^{\max} = \max_{S_i}(E) \quad (7)$$

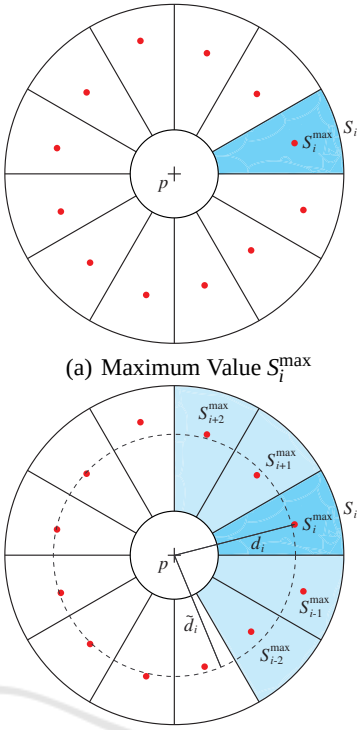

(a) Maximum Value $S_i^{\max}$

(b) Distance d_i

Figure 2: Outline to Generate Likelihood Map.

Next, position of obtained $S_i^{\max}$ is obtained as $p_{S_i}^{\max}$. Euclid distance d_i is calculated between p and $p_{S_i}^{\max}$ as shown in Fig.2(b).

Median of the distance d is obtained in the region S_i with its front and rear regions.

$$\tilde{d}_i = \mathrm{median}(d_j) \quad j \in \left[i - \frac{l-1}{2}, \cdots, i + \frac{l-1}{2} \right] \quad (8)$$

where l is the number of regions when median is calculated. Weight γ_i is calculated from Eq.(9) using distances d_i and $\tilde{d}_i$.

$$\gamma_i = \frac{1}{1 + \frac{|d_i - \tilde{d}_i|}{\tilde{d}_i}} \quad (9)$$

where γ_i becomes larger when the distance d between interesting pixel p and the maximum value $S_i^{\max}$ becomes similar for the sequential regions since the maximum value $S_i^{\max}$ is judged as part of edge of a circle.

Next, α_i is obtained from Eq.(10) using mean of $(R_{d_i > d_i})$ and value of R component (R_p) of interesting pixel whose distance has larger than the distance d_i.

$$\alpha_i = \frac{R_p}{\mathrm{mean}\,(R_{d_i > d_i})} \quad (10)$$

Weight α'_i is obtained by applying sigmoid function to the obtained α_i. α'_i becomes larger when intensity of interesting pixel is larger than mean value of surrounding pixels, while smaller for the inverse case. Inside of polyp becomes brighter and outside becomes darker in endoscope image. Edge may be part of polyp if weight α'_i takes larger value, while it may be part of inner lining if α'_i takes smaller value.

Next, $\hat{S}_i^{\max}$ is obtained by multiplying the maximum value $S_i^{\max}$, weight of distance γ_i and weight of color α'_i.

$$\hat{S}_i^{\max} = \alpha'_i \gamma_i S_i^{\max} \tag{11}$$

Finally, the median MS_p of $\hat{S}_i^{\max}$ obtained for each region is obtained.

$$MS_p = \text{median}_i(\hat{S}_i^{\max}) \qquad i \in [1, \cdots, n] \tag{12}$$

where n is the divided number of a circle. Obtained MS_p is used as value of likelihood map corresponding to the interesting pixel. Candidate region is extracted from the region which has more than 80 percentages of the maximum value of generated likelihood map. This threshold is obtained from the experience of many trials. Size of candidate region is determined by the distance $d_{\max}$ between the interesting pixel and maximum edge intensity inside a judgement circle. Rectangle with a side $2d_{\max}$ whose center is located at an interesting pixel is extracted as a candidate region.

2.4 Classification by Random Forests

Paper (Iwahori et al., 2013) uses SVM with feature selection and boosting is applied to construct a strong classifier. As boosting tends to be sensitive to noise data, the proposed approach uses random forests (Breiman, 2001) which is more robust to the noise data. Random Forests is introduced to construct classifier with high accuracy by combining low correlated weak classifiers. Random forests use decision trees as weak classifiers.

The whole learning data is $\vec{S}$ is learned with learning data $\vec{S_0} \in \vec{S}$ which is randomly selected for each decision tree. Node of the learning data $\vec{S_0}$ allows the overlapping of data. Split function at node j of learning data $\vec{S_0}$ is given by Eq.(13).

$$h(\vec{v}, \theta_j) \quad \in \quad \{0, 1\} \tag{13}$$

$\vec{v}$ represents data which reached node j, and θ represents the parameter to decide the split function, where $\theta=(\phi, \psi, \tau)$. ϕ means the filter which extracts several features from d-dimensional data $\vec{v}$, ψ means the splitting criteria and τ means the threshold for the split. Decision tree is constructed until data splitting cannot be done anymore.

The input data v is input to all decision trees in classification by Random forests as shown in Fig.3. In each decision tree, it is decided which to proceed to either the left or right child node according to the split function h assigned to the node, and eventually reaches the leaf node Classification is done by a majority vote of the result obtained by each decision tree. The result is obtained by converging posterior probability derived each decision tree with the following Eq.(14), where $p_t(c|v)$ is the predicted value of the a posteriori probability obtained by the t-th decision tree.

$$p(c|v) = \frac{1}{T} \sum_{t=1}^{T} p_t(c|v) \tag{14}$$

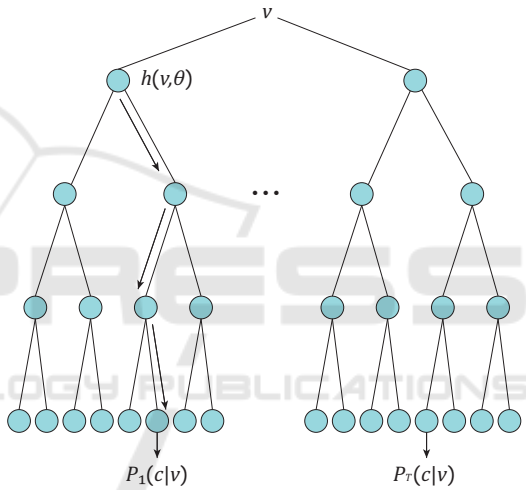

Figure 3: Random Forests.

2.5 Integration of Detected Results

When the approach is applied for the detection of polyp in endoscope image, multiple rectangles for polyp candidate are detected. Here k-means++ (Arthur and Vassilvitskii, 2007) is used to integrate the detection results for improving accuracy.

k-means++ is an algorithm to find the cluster center. Cluster center corresponds to the point which minimizes the variance inside classes, in other words, the point which minimizes the squared sum of distance between the point and each data point inside a class. k-means++ is an improvement of k-means. Point is randomly selected and cluster center is determined. After that, data which have not been selected to cluster center become cluster center with the probability which is proportional to the distance between its nearest neighbor cluster center and all data.

Algorithm of integrating detected results is shown as follows.

Step1. Data are randomly selected and initial point is determined at the center of clusters $\vec{C}_1$

Step2. Distance $D(x_i)$ between data and center of clusters $\vec{C}_j$ to which the data belong is calculated.

Step3. Let $\frac{D(x_i)^2}{\sum_i^N D(\vec{x}_i)^2}$ be the weight, and the data which are more than random threshold at first is selected and assigned as the center of cluster.

Step4. Class $\vec{L}$ which belongs to all data is calculated again.

Step5. Repeat **Step2** to **Step4** until number of clusters becomes k.

Step6. k-means is applied to the center of clusters $\vec{C}$ obtained by **Step5** as an initial point.

Step7. If the distance between resulting clusters of k-means is less than the threshold, let $k = k - 1$ and start from **Step1**.

Center of clusters for detected result is calculated by k-means++ and each cluster is represented as a rectangle. Size of rectangle is taken as the median of sizes of candidate regions judged as the same cluster. Detected rectangles are integrated by k-means++ and integrated result is shown in Fig.4.

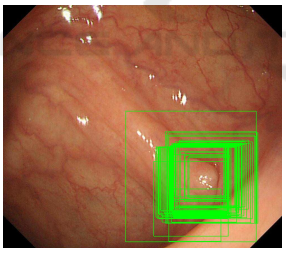

(a) Before Integration

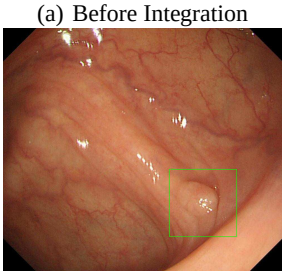

(b) After Integration

Figure 4: Integrated Result.

3 EXPERIMENTS

Experiment is demonstrated to confirm the usefulness of the proposed approach in comparison with the paper (Iwahori et al., 2013) and paper (Bernal et al., 2015). Edge detection to extract candidate region and obtained likelihood map using the edge are compared with that of paper (Bernal et al., 2015). Next, accuracy with classifier applied for the candidate region is evaluated with paper (Iwahori et al., 2013).

3.1 Edge Detection

Fig.5 and Fig.6 shows the original image, edge image obtained by paper (Bernal et al., 2015) and proposed approach respectively. Here, color close to red represents the strong edge intensity, while color close to blue represents the weak edge intensity. Fig.5 shows the image without blood vessel, while Fig.6 shows the image with blood vessel.

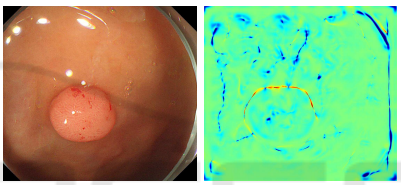

(a) Original Image (b) Paper(Bernal et al., 2015)

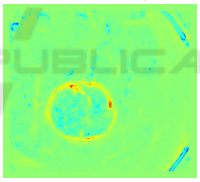

(c) Proposed Approach

Figure 5: Edge Detection 1.

It is shown that edge of polyp is detected by both of paper (Bernal et al., 2015) and proposed approach from Fig.5. While paper (Bernal et al., 2015) detects edge of blood vessel from Fig.6 and proposed approach reduces edge of blood vessel. It is shown that edge detection by proposed approach reduces the detection of blood vessel and this is clear advantage of the proposed approach.

3.2 Likelihood Map

Fig.7 and Fig.8 show the likelihood map obtained by paper (Bernal et al., 2015) and that by the proposed approach for the comparison.

Likelihood map represents that color close to red has the high possibility of polyp, while color close

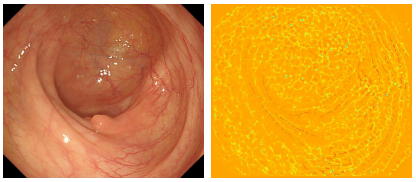

(a) Original Image (b) Paper (Bernal et al., 2015)

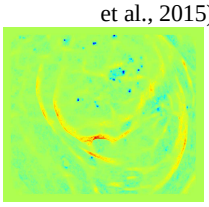

(c) Proposed Approach

Figure 6: Edge Detection 2.

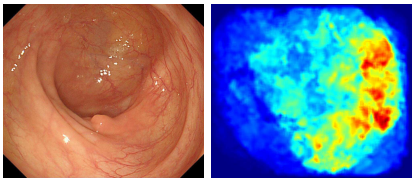

(a) Original Image (b) Paper (Bernal et al., 2015)

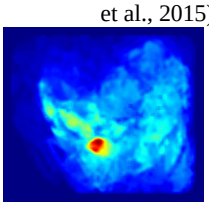

(c) Proposed Approach

Figure 8: Likelihood Map 2.

to blue has the low possibility of polyp, respectively. Here the radius of judgement circle was 150 pixels, divided angle of judgement circle was 30 degrees and l to obtain the distance $\tilde{d}_i$ was 5. Pixels within the radius 10 pixels around interesting pixel was for out of calculation. This is done to reduce the incorrect detection for interesting pixel which has high likelihood on the strong edge or around the edge.

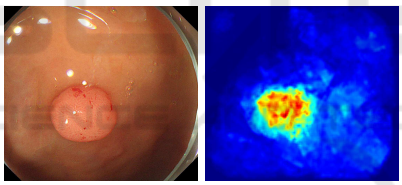

(a) Original Image (b) Paper (Bernal et al., 2015)

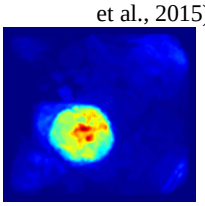

(c) Proposed Approach

Figure 7: Likelihood Map 1.

Fig.7 shows that large values are obtained on polyp when there is no blood vessel in an image, while paper (Bernal et al., 2015) gives large value around blood vessel in Fig.8 when blood vessel exists in an image. While the proposed approach gives large value on polyp in both cases and stable results are obtained. This is because paper (Bernal et al., 2015) assumes that region surrounded by the edge is polyp and when there are many blood vessels, likelihood becomes high value. While the proposed approach tends not to detect blood vessel as edge, and the proposed approach has advantage for detection of candidate region of polyp. Next, weight of color was confirmed for the usefulness. Fig.9 shows likelihood map with weight of color and that without weight of color.

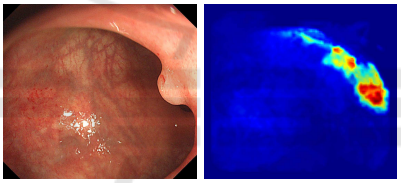

(a) Original Image (b) Map without Weight of Color

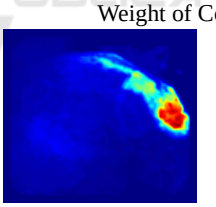

(c) Map with Weight of Color

Figure 9: Weight of Color.

Fig.9 shows that weight of color is also useful since inner edge has small value and polyp has large value. When weight of color is not used, it is shown that inner edge has large value of map.

3.3 Evaluation of Accuracy

Learning data set used in the experiment is around 2400 pixel for small image data to around 240000 pixels for large image data. Resolution and number of polyp images are around 1100 $\times$ 1000 pixels and 154 images. Test data set used is a total of 440 images with 1000 $\times$ 869 pixels from three endoscope

videos. Mask image of polyp is prepared by manual operations and used to judge whether detected region is polyp or not. As an approach of paper (Iwahori et al., 2013), strong classifier is constructed by Adaboost using each SVM after applying feature selection as a weak classifier. Parameters of SVM were determined by the grid search. Number of trees of random forests was set to be 500 in the proposed approach.

Sensitivity, Specificity and Accuracy were calculated using the following equations as the evaluation of classification, where sensitivity represents the correct ratio of polyp region, specificity represents the correct ratio of non-polyp region, and accuracy represents the correct ratio for whole test samples.

$$Sensitivity = \frac{Number\ of\ Correct\ Positive\ Predictions}{Number\ of\ Positives} \quad (15)$$

$$Specificity = \frac{Number\ of\ Correct\ Negative\ Predictions}{Number\ of\ Negatives} \quad (16)$$

$$Accuracy = \frac{Number\ of\ Correct\ Predictions}{Number\ of\ Positives + Number\ of\ Negatives} \quad (17)$$

Evaluation was done using endoscope movie taken in 3 different scenes. The result is shown in Table 1. Here, proposed approach is run for five times and its mean was used for the evaluation result considering randomness of the approach. Upper line of each criteria shows evaluation by Paper (Iwahori et al., 2013) and lower line of each criteria shows evaluation by proposed approach.

Table 1: Evaluation of Accuracy [%].

	Scene 1	Scene 2	Scene 3	Total
Sensitivity	59.83	92.86	19.89	38.00
	77.58	94.61	96.67	81.68
Specificity	78.65	81.32	77.38	77.70
	55.71	66.02	81.57	78.22
Accuracy	77.83	81.44	76.89	77.22
	76.31	78.32	83.08	79.84

Table 1 suggests that proposed approach gives higher sensitivity but lower specificity than paper (Iwahori et al., 2013). Important goal is not to fail in detection of polyp and approach with higher sensitivity has usefulness in polyp detection.

Each result of five trials of proposed approach is shown in Table 2.

Proposed approach has randomness but it is confirmed that five times trials gives polyp detection with almost the same level of accuracy.

Detected result by paper (Iwahori et al., 2013) is shown in Fig.10 and that by proposed approach is shown in Fig.11. Here, the region with green color is the resulting region recognized as polyp. Proposed approach represents an integrated result with detected rectangles.

Table 2: Evaluation of Accuracy in Each Trial [%].

		Sensitivity	Specificity	Accuracy
1st	Scene 1	77.24	56.41	76.04
	Scene 2	95.31	65.82	78.51
	Scene 3	97.20	80.18	81.89
2nd	Scene 1	78.48	53.53	77.04
	Scene 2	94.22	68.64	79.65
	Scene 3	97.20	81.94	83.47
3rd	Scene 1	81.41	49.36	79.56
	Scene 2	96.15	62.45	76.95
	Scene 3	96.47	80.92	82.48
4th	Scene 1	75.46	57.69	74.43
	Scene 2	95.19	63.27	77.01
	Scene 3	96.17	80.74	82.29
5th	Scene 1	75.30	61.54	74.51
	Scene 2	92.18	69.91	79.49
	Scene 3	96.32	84.07	85.30

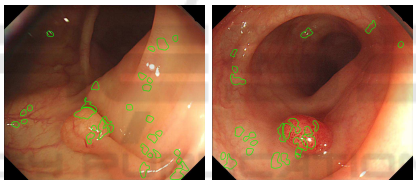

(a) Scene1 (b) Scene2

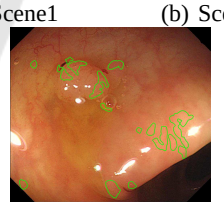

(c) Scene3

Figure 10: Detected Result of Paper (Iwahori et al., 2013).

Fig.10 and Fig.11 show that approach of paper (Iwahori et al., 2013) detects part of polyp but proposed approach detects most part of polyp with better detection. This is because the proposed approach uses the distance to the edge to recognize a size of polyp candidate region.

4 CONCLUSION

This paper proposed a novel approach to detect polyp region automatically. The approach first detects the polyp candidate region based on the likelihood map

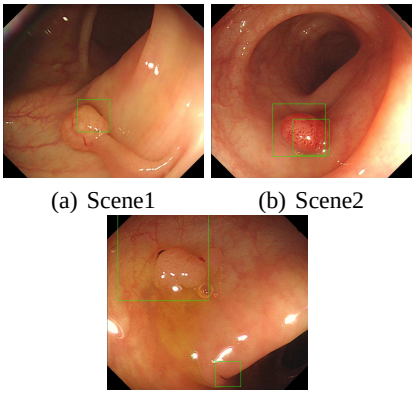

(a) Scene1 (b) Scene2

(c) Scene3

Figure 11: Detected Result of Proposed Approach.

using both of edge information and color information of endoscope image. After detecting the candidate region, random forests were applied to judge polyp region automatically.

It is shown that the proposed approach gives higher performance through the experimental evaluations. Further subjects include further improvement of accuracy by adding different combination of features and improvement of processing speed.

ACKNOWLEDGEMENT

Iwahori's research is supported by Japan Society for the Promotion of Science (JSPS) Grant-in-Aid for Scientific Research (C) (26330210) and by a Chubu University Grant. The authors also thank lab. member for their useful discussions.

REFERENCES

Alexandre, L., Nobre, N., and Casteleiro, J. (2008). Color and position versus texture features for endoscopic polyp detection. In *International Conference on BioMedical Engineering and Informatics (BMEI 2008), Vol.2, pp.38-42*.

Ameling, S., Wirth, S., Paulus, D., Lacey, G., and Vilarino, F. (2009). Texture-based Polyp Detecion in Colonoscopy. In *Springer Berlin Heidelberg New York, pp.346-350*. Springer.

Arthur, D. and Vassilvitskii, S. (2007). k-means++: The Advantages of Careful Seeding. In *Proceedings of the 18th annual ACM-SIAM symposium on Discrete algorithms, Society for Industrial and Applied Mathematics, pp.1027-1035*.

Bernal, J., Sanchez, F., G.F-Esparrach, Gil, D., Rodriguez, C., and Vilarino, F. (2015). WM-DOVA maps for accurate polyp highlighting in colonoscopy: Validation vs. saliency maps from physicians. In *Computerized Medical Imaging and Graphics, Elsevier, Vol.43, pp.99-111*.

Breiman, L. (2001). Random forests. In *Machine Learning, Vol.45, No.1, pp.5-32*.

Hwang, S., Oh, J., Tavanapong, W., Wong, J., and deGroen, P. (2007). Polyp detection in colonoscopy video using elliptical shape feature. In *International Conference on Image Processing, Vol.2, pp.465-468*. IEEE.

Iakovidis, D., Maroulis, D., Karkanis, S., and Brokos, A. (2005). A comparative study of texture features for the discrimination of gastric polyps in endoscopic video. In *Proceedings of 18th IEEE Symposium on Computer-Based Medical Systems, pp.575-580*.

Iwahori, Y., Shinohara, T., Hattori, A., Woodham, R., Fukui, S., Bhuyan, M., and Kasugai, K. (2013). Automatic Polyp Detection in Endoscope Images Using a Hessian Filter. In *Proceedings of MVA 2013, pp. 21-24*. IAPR.

Karkanis, S., Iakovidis, D., Maroulis, D., Karras, D., and Tzivras, M. (2003). Computer-aided tumor detection in endoscopic video using color wavelet features. In *IEEE Transactions on Information Technology in Biomedicine, Vol.7, No.3, pp.141-152*. IEEE.

Li, B. and Meng, M. (2011). Comparison of Several Texture Features for Tumor Detection in CE Images. In *Journal of Medical Systems, Vol.36, No.4, pp.2463-2469*.

Shen, H. and Cai, Q. (2009). Simple and efficient method for specularity removal in an image. In *Applied Optics, Optical Society of America, Vol.48, No.14, pp.2711-2719*.